Carbon 164 (2020) 12–18

Contents lists available at ScienceDirect

Carbon

journal homepage: www.elsevier.com/locate/carbon

A metal free electrocatalyst for high-performance zinc-air battery applications with good resistance towards poisoning species

Tayyaba Najam [a, b], Syed Shoaib Ahmad Shah [c, ***], Hassan Ali [d], Zhaoqi Song [a], Haohao Sun [a], Zhengchun Peng [b, **], Xingke Cai [a, *]

[a] Institute for Advanced Study, Shenzhen University, Shenzhen, 518060, China
[b] Key Laboratory of Optoelectronic Devices and Systems of Ministry of Education and Guangdong Province, College of Physics and Optoelectronic Engineering, Shenzhen University, Shenzhen, 518060, China
[c] Department of Chemistry, The Islamia University of Bahawalpur, 63100, Pakistan
[d] Department of Chemistry, Tsinghua University, Beijing, China

ARTICLE INFO

Article history:
Received 5 February 2020
Received in revised form
4 March 2020
Accepted 16 March 2020
Available online 19 March 2020

Keywords:
Metal-free electrocatalyst
Dual-doped carbon
Oxygen reduction reaction
Antipoisoning effect
Zinc-air battery

ABSTRACT

The trace amount of poisoning species in air, such as SO_x and NO_x, greatly degrade the performance of zinc-air battery, as they block the active sites of conventional metal containing electrocatalysts. To overcome this challenge, a catalyst with enhanced electrocatalytic properties and good resistance towards the small molecular poisons should be prepared. In this work, we synthesized a P, N dual-doped porous carbon nanospheres (DDPCN), which showed an E_{onset} and $E_{1/2}$ of 0.98 V and 0.87 V for ORR reduction in alkaline solution, and a Tafel slop of 72 mV/dec, over-performing all the other metal-free catalysts and comparable with the performance of state-of-the-art Pt/C (20 wt%). Moreover, the $E_{1/2}$ for DDPCN showed negligible change towards poisoning species; while the $E_{1/2}$ for Pt/C and typical CoO_x/CNTs displayed 10/10 mV and 24/13 mV decay by adding trace amount of SO_3^{2-}/NO_2^- into the electrolyte solution. By using DDPCN as the electrocatalyst for zinc-air battery application, the device showed the highest open circuit voltage (1.48 V), the highest power density (224 mW cm^{-2}) and the highest energy density (874 W h kg^{-1}) among all metal-free catalysts, and their performances are even better than the Pt/C catalyst. Moreover, these performances showed negligible influence by the poisoning species for DDPCN based Zn-air battery, while the performances for Pt/C and CoO_x/CNTs based Zn-air batteries were greatly deteriorated by the poisoning species up to 25% and 40%.

1. Introduction

Metal-air batteries are considered as a promising device among various renewable energy storage systems [1–4]. Among them, zinc-air batteries have become foci of research due to their great theoretical energy density (1084 Wh kg^{-1}), low cost as well as environmental benignity [5–11]. Currently, the main problem for the zinc-air battery is the lack of a superior electrocatalyst to promote the oxygen related reaction in the cathode. The ideal catalyst needs to show comprehensive performances, including low overpotential for oxygen related reaction in alkaline solution, long term stability, good resistance towards the environmental poisoning, low cost and mass production [12].

By far, a lot of materials have been used to promote oxygen related reaction in the alkaline solutions, such as precious metal/metal oxides, non-precious metal-based catalysts (NPMCs, Fe/Co-N_x-C, layered double hydroxides, oxides, *etc.*) and non-metallic carbon materials [3,13–15]. Among them, precious metal catalysts (PMCs), such as Ru, Ir, Pt, and their alloys stand to be the best choice for oxygen related reactions, which show very low overpotential and low slop of Tafel plots [16–18]. However, their real uses are limited by their scarcity, poor durability, high cost, and low resistance towards poisoning species (SO_x, NO_x, PO_x) [19,20]. NPMCs are considered as the possible alternative to PMC as they show excellent electrocatalytic performance in alkaline solutions [13,21,22]. Nevertheless, several problems degrade the stability of NPMCs, such as the production of H_2O_2, and the proton/anion binding [23–28]. In the meantime, their performances would also be

* Corresponding author.
** Corresponding author.
*** Corresponding author.
E-mail addresses: shoaib03ahmad@outlook.com (S.S. Ahmad Shah), zcpeng@szu.edu.cn (Z. Peng), cai.xingke@szu.edu.cn (X. Cai).

https://doi.org/10.1016/j.carbon.2020.03.036
0008-6223/

greatly deteriorated by the adsorbed poisoning species in the solution [29,30]. The small molecules, such as SO_x and NO_x, have a strong interaction with the metallic active sites, and tend to block them. Therefore, the poisoning effect is the common problem for both precious metal and non-precious metal-based catalysts to satisfy all the requirements for zinc-air battery applications.

The metal-free carbon materials without the metal catalytic centers may be much less influenced by the trace amount of toxic small molecules in air. The main problem for this type of catalysts is their sluggish reaction kinetics due to low activity of catalytic sites. Recent studies revealed that doping of nonmetallic elements, such as P, B, S, and N, into the carbon materials greatly tuned the electronic and physicochemical properties of carbon materials, improving their electrocatalytic activity [31–37]. Among them, the nitrogen dopants in carbon showed an active role for ORR [37–39]. In the meantime, theoretical analysis indicated that co-doping of nonmetallic elements will further enhance the ORR performance [40]. P, N co-doping are particularly attractive for ORR as they induced defects that can lead to highly localized state nearby Fermi level [37,40]. The doping of P creates a lot of defects in carbon framework which would benefit the doping of nitrogen to form P and N co-doped structure during the pyrolysis. The larger atomic size and lower electronegativity of P than N lead to better adsorption of oxygen through occupying the vacant 3d orbitals of P/N by valence electrons [41]. Therefore, the co-doping of N and P into the carbon materials may show excellent performance for ORR in alkaline solution with good resistance towards the poisoning species, such as NO_x and SO_x.

Herein, we prepared a porous P, N dual-doped carbon nanospheres (DDPCN) with plenty of edges through a highly modest and fast polymerization and pyrolyzing route with gram quantities. The DDPCN electrocatalyst shows superior ORR-activity in 0.1 M KOH with 0.98 V and 0.87 V of onset and half-wave potentials (E_{onset} and $E_{1/2}$), better than any other reported nonmetallic catalysts. When the DDPCN was used as electrocatalysts for O_2-cathode for zinc-air battery application, it exhibited 224 mW cm^{-2} of peak power density, 786 mA h g^{-1} of specific capacitance at 20 mA cm^{-2} and long-term stability, better than the state-of-the-art Pt/C (20%). Moreover, it displayed great tolerance towards SO_x and NO_x while Pt/C (20%) and CoO_x/CNTs showed drastic performance degradation towards these poisoning species.

2. Result and discussion

The DDPCN was synthesized by a polymerization and pyrolysis procedure as our previously reported method with some modifications [42]. The stable and uniform spherical poly-diaminopyridine (PDAP, ~300 nm in diameter) particles with high percentage of nitrogen dopants, were synthesized via polymerization of diaminopyridine (DAP, Fig. 1a). Then, P-source was added onto the surface of PDAP to form P-doped poly-diaminopyridine (P-PDAP) through self-assembly procedure with a phytic acid/PDAP molar ratio of 8/1. Finally, the P-PDAP was pyrolyzed at 1000 °C in nitrogen gas to get the DDPCN.

We firstly characterized the structure and morphology of as-prepared DDPCN. The scanning electron microscopic (SEM) images indicated that P-PDAP inherited the uniform spherical structures (Fig. 1b–c). After pyrolysis procedure, the surface of as formed DDPCN was slightly contracted. As shown in TEM images (Fig. 1d–e), the as formed DDPCN possesses edge-like porous structures, which should be beneficial for enhancing the catalytic properties.

The N_2 sorption isotherms were then used to analyze the pore structure and the corresponding surface area of as-synthesized products. All the materials showed a steep N_2 gas uptake curves in low pressure region, which is the characteristic feature of isotherm Type-IV [43], specifying the mesoporous nature with pore size around 4–6 nm (Fig. 2a–b). The observed specific area (894 m^2 g^{-1}) of DDPCN (1000 °C) is much higher than that of 687 and 179 m^2 g^{-1} for nitrogen doped carbon (CN) and phosphorous doped carbon (CP) (supporting information, Table S1). This result means that the co-doping of N and P produced more defective sites in DDPCN than single dopants of N or P in the carbon material, which should also be the reason for larger surface area of DDPCN than CN and CP. Therefore, we concluded that a defective spherical DDPCN with 4–6 nm porous structure inside was obtained, which showed very high specific surface area. In principle, such a conductive mesoporous carbon material should be beneficial for the electrons and mass transportation during the gas-related electrocatalytic process.

X-ray photoelectron spectroscopy (XPS) was used to analyze the composition and bonding structure of N and P in DDPCN (Fig. 2c–f). The survey XPS analysis demonstrated that doping of P increased the N and O contents in C from 2.18 wt% and 3.81 wt% to 2.92 wt% and 4.47 wt% in the DDPCN, while the contents of P remains same as in CP. According to previous study, oxygen has no influence on the final electrical performance [42]. Compared to CN and CP, the increased oxygen contents in DDPCN should be due to better absorption of co-doping strategy. The main difference of N1s spectra for CN and DDPCN is the increased contents (atomic %) of pyridinic-N from 25% to 37% after P doping, and the carbon atoms connected to them are claimed to be the main active sites for the ORR [44]. For P2p spectra (Fig. 2f), the peak width for DDPCN was much broader than CP, which was due to the formation of P–C–N bonding structure because of N-doping, except the P–O and P–C bonds. Therefore, compared with CN and CP, the DDPCN has a higher amount of pyridinic N and a newly formed P–C–N bonding structure, which is the main difference from the CP and CN.

The ORR performance of as-synthesized electrocatalysts were monitored in an alkaline solution with 0.1 M KOH by rotating disk electrode (RDE) and rotating ring disk electrode (RRDE) test. Based on RRDE-LSV results (Fig. 3a), DDPCN and Pt/C (20%) showed a similar onset potential (E_{onset}) of 0.98 V vs RHE and diffusion limiting current density of ~5.2 mA/cm^2. While CN and CP showed very low E_{onset} values of 0.77 and 0.65 V and low current densities of 4.16 and 2.16 mA/cm^2 at 0.4 V. Furthermore, the half-wave ($E_{1/2}$) potential of DDPCN (0.87 V) is similar to Pt/C (0.87 V), however far greater than CN (0.73 V) and CP (0.55 V). This further confirmed that dual-doping strategy is more effective to enhance ORR performance. To understand the ORR pathway, the electron transferred number (n) of the catalysts were calculated at different voltage based on the equation of $n = 4I_{disk}/(I_{disk}+1/2I_{ring})$ (Fig. 3b). The value n for DDPCN was above 3.9 at any applied voltage (0.2–0.7 V *vs* RHE), a little bit higher than the Pt/C, much better than the CN and CP, indicating the efficient reduction of oxygen to OH^- by DDPCN through 4 e′ pathway. The peroxide production for DDPCN was < 3%, slightly lower than that for Pt/C (>4%), but much lower than that for CP and CN (~25%). The Tafel slope shown in Fig. 3c revealed 76, 74, 115 and 139 mV/dec for the Pt/C, DDPCN, CN and CP, respectively. Additionally, the stability of DDPCN and Pt/C (20%) were investigated by CV-cycling test between 0.6 and 1.2 V (RHE) at a sweeping rate of 50 mV/s in 0.1 M KOH (Fig. 3d). After 10,000 CV-cycles, the DDPCN showed only 5 mV decrease in $E_{1/2}$, in contrast $E_{1/2}$ difference of 20 mV was displayed by Pt/C. Therefore, all these features confirmed the DDPCN as a good ORR catalyst in alkaline medium, even slightly better than Pt/C (20%). When compared with the reported results by using the metal-free catalysts for ORR in alkaline medium (Table S3), the DDPCN even showed the best comprehensive performance.

The good performance of DDPCN could be understood from the

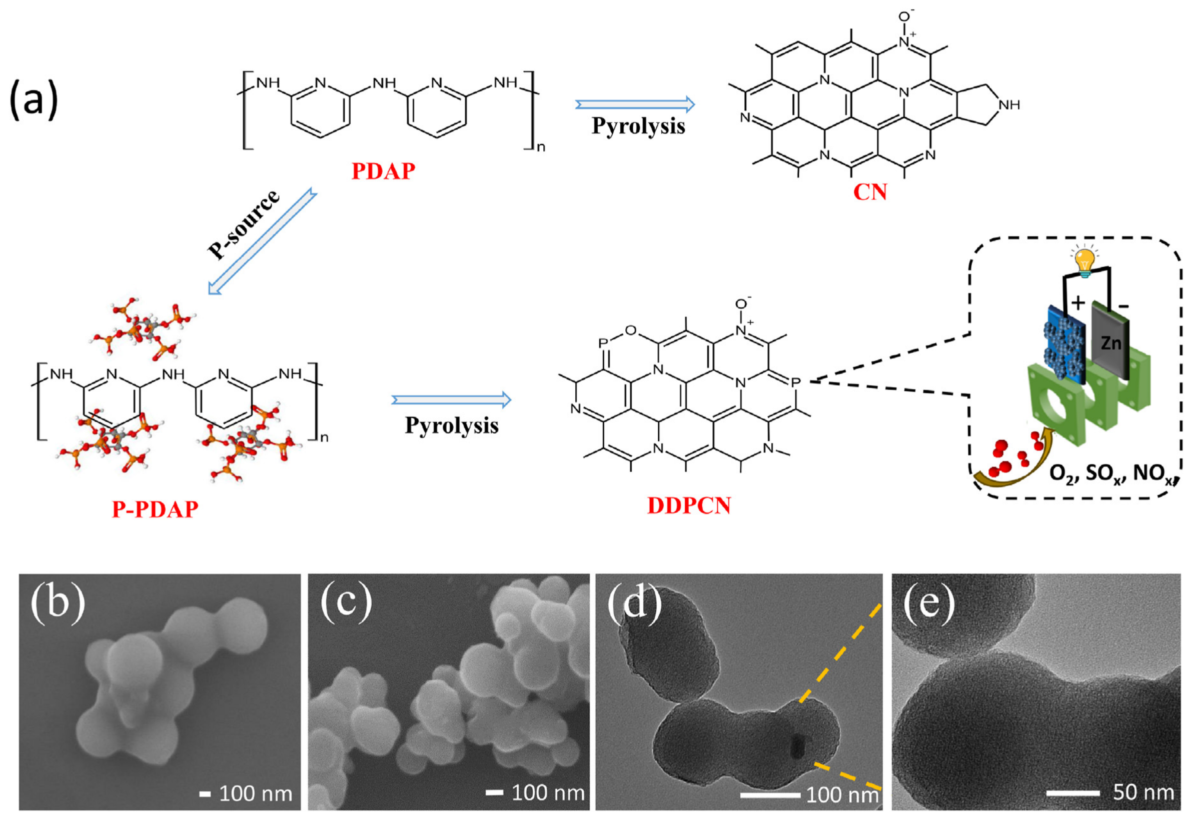

Fig. 1. (a) Schematic illustration for the synthesis of DDPCN, (b–c) SEM images of P-PDAP & DDPCN, (d–e) TEM images of DDPCN. (A colour version of this figure can be viewed online.)

microstructure and the bonding structure difference from the CN. First, compared with nitrogen doped carbon, P, N dual doping showed a much larger surface area due to the defects, which means more active sites were exposed to the O_2. Second, the P doping increased the contents of N from 2.18% to 2.92% inside the carbon materials and the ratio of active pyridinic N from 25 atm% to 37 atm %. The carbon atoms close to pyridinic N in carbon materials are claimed to show excellent catalytic properties in alkaline solution. In addition, the optimized P/N ratio in the carbon substrate should also have a big influence on the ORR performance of DDPCN. We have prepared the DDPCN with different phytic acid/PDAP molar ratio, and the ORR activity of all these catalysts were much better than the CN and CP (Fig. S2). Among them, the phytic acid/PDAP ratio of 8/1 was the optimized ratio, which showed the best ORR performance rather the one with the highest phosphorous contents. The possible reason is that the over-doped P atoms may destroy the original P, N co-doped carbon framework, leading to a decreased activity for ORR. Therefore, the great ORR property in the DDPCN should be ascribed to the high content of pyridinic carbon, the large specific surface area and optimized heteroatom doping strategy.

The performance degradation due to the presence of small molecules or radicals is a main challenge for the use of many conventional metal containing catalysts, such as the Pt/C and CoO_x/CNT [20,24,28,30]. We studied the anti-poisoning effect of the metal-free DDPCN towards small molecular poisons like SO_x and NO_x in 0.1 M KOH (Fig. S3). The Pt/C and CoO_x/CNT (prepared according to our previously reported method [3]) were used as comparison catalysts. The DDPCN catalyst exhibited almost no activity decrease in the presence of SO_3^{2-} (50 mM) and NO_2^- (50 mM) while drastic performance loss was shown by Pt/C (20%) and CoO_x/CNTs. The highest degradation was detected in case of SO_x by Pt/C and CoO_x/CNTs with $E_{1/2}$ decay of 10 mV and 25 mV, respectively. The probable cause for activity loss was due to the strong adsorption of poisoning species on the surface of catalysts, which tends to block the metallic active sites [28–30,42]. Since previous reported results indicated the poisoning effect on the nitrogen doped carbon materials [19,29], the excellent resistance towards SO_x and NO_x for DDPCN in the alkaline solution should be related with the newly formed P–C–N bonding structure. Our previous studies identified the preferred locations of NO_x and SO_x molecules on the surface of these nonmetallic catalysts by analyzing the distribution of relative electron concentration along graphene model surface [42]. The NO_x and SO_x molecules tend to adsorb on carbon atoms near the P/N atoms for CP and CN. As shown in Fig. 4, the high transfer of electrons from carbon to P and N in purely P-doped carbon and N-doped carbon, lead to the strong polarization of the P–C and N–C bonds. The positively charged carbon sites tend to adsorb the anionic SO_3^{2-} and NO_2^- on them, blocking the active sites. For the co-doped carbon material, the doped P atoms would introduce defects nearby and the N atoms would take up these positions, which means the active carbon site were connected with one P and one N atom. This carbon site is the active sites for ORR reactions, which needs to give electrons to both the P and N atom, leading to a balanced polarization [42]. This result means the anionic poison species in the solution would have lower tendencies to deposit on the carbon material. The repulsion force of the P and N atoms from both sides to the anionic poison species protected the carbon atoms from being blocked. Hence, P, N co-doping played a crucial role for maintaining the durability and tolerance of the DDPCN catalyst.

Motivated by the superior ORR activity, the DDPCN was used as the cathode catalyst for Zn-air battery application (Fig. 5). First, the

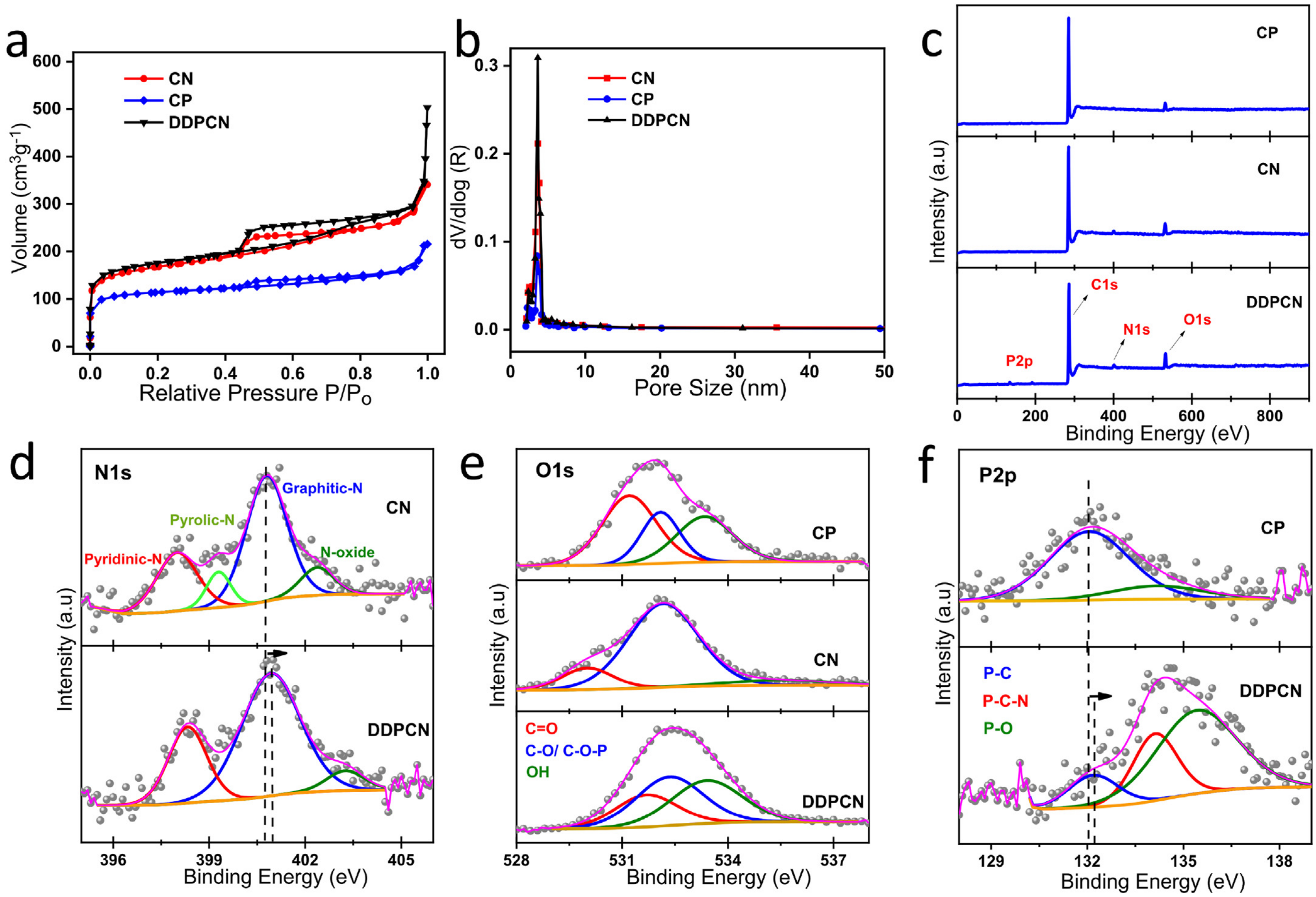

Fig. 2. (a) Comparative analysis of N_2 adsorption–desorption isotherms, (b) Pore size distribution of CN, CP, DCPN, (c) XPS survey spectrum of PC, DDPCN, NC; High-resolution XPS spectra (d) N1s, (e) O1s & (f) P2p. (A colour version of this figure can be viewed online.)

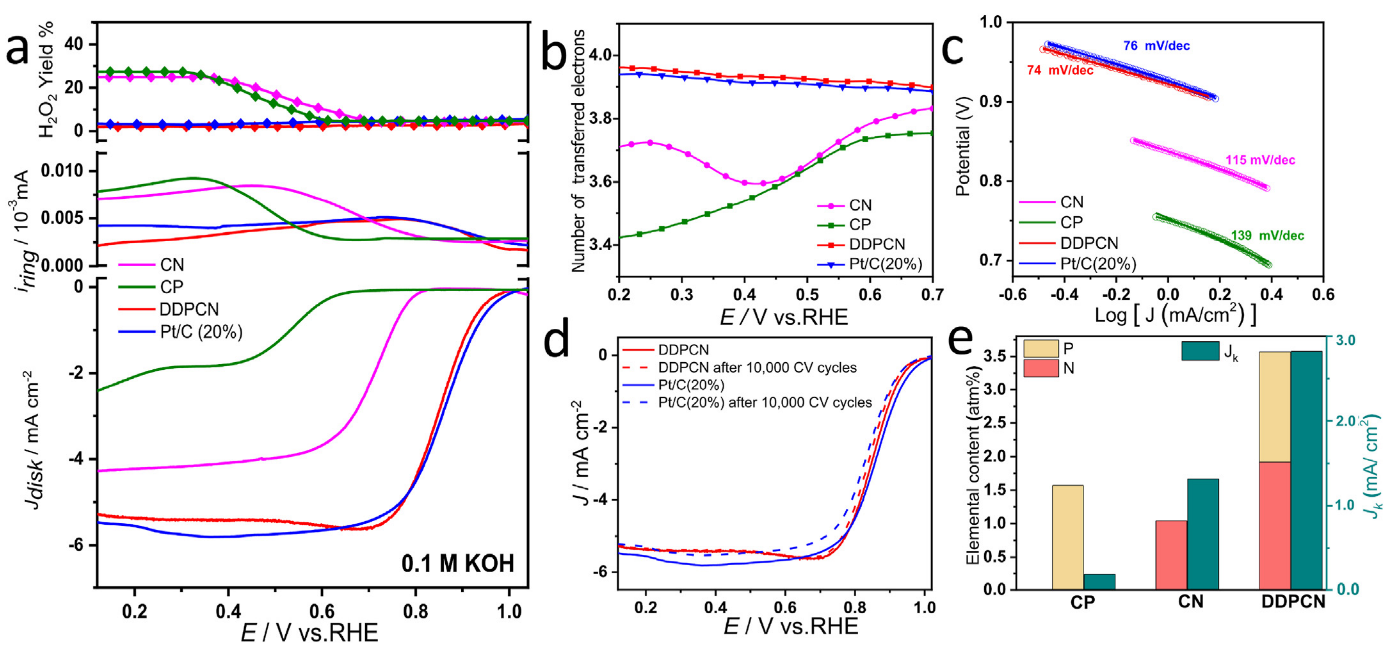

Fig. 3. (a) LSV comparison Plot at 1600 rpm in 0.1 M KOH and peroxide%, (b) The number of transferred electrons, (c) Tafel plot, (d) ORR stability test of Pt/C (20%) & PNC in 0.1 M KOH, (e) The J_k value calculation from ORR-LSV curves and elemental content derived from XPS analysis. (A colour version of this figure can be viewed online.)

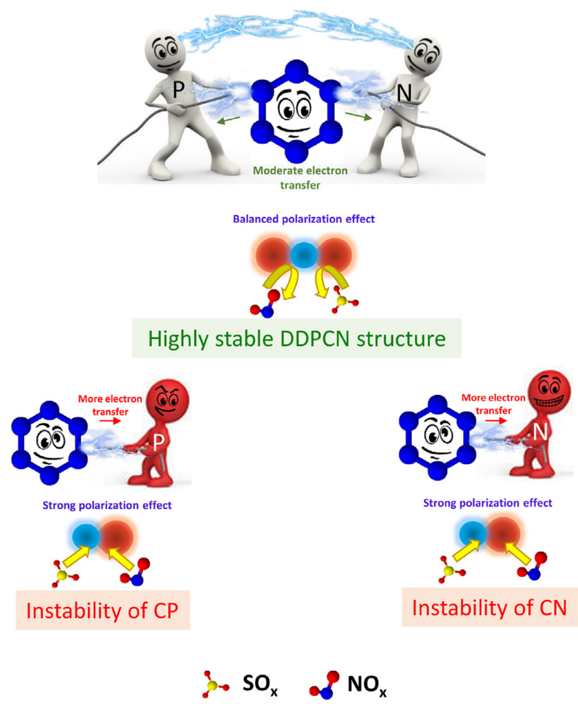

Fig. 4. Schematic illustration for the structural resistance of DDPCN, CN, and CP for the incoming small molecules NO_x and SO_x.(A colour version of this figure can be viewed online.)

key performance parameters for Zn-air battery, such as power density, energy density, open circuit voltage, have been studied. The commercially used Pt/C (20%) catalyst was taken as a reference. As shown in Fig. 5a, the peak power density for DDPCN was 224 mW/cm^2, similar to that of Pt/C (223 mW/cm^2). In the meantime, the specific capacity for DDPCN, and Pt/C were 786 mA h/g, and 725 mA h/g by normalizing the consumed zinc mass at a current density of 20 mA/cm^2 (Fig. 5b). The open circuit voltage of 1.48 V for Zn-air battery was produced with DDPCN electrode and 874 Wh/kg of energy density at 10 mA/cm^2 was obtained, thus comparatively higher than other reported non-previous metal based electrocatalysts (Fig. S5 and Table S4). The stability of the catalysts was examined by galvanostatic charge-discharge cycling test at 20 mA/cm^2 (Fig. 5c). The DDPCN catalyst showed excellent stability by preserving the charge-discharge voltage gap even after 30 h whereas Pt/C (20%) revealed drastic stability loss by increasing charge-discharge voltage gap. As shown in Fig. 5d, the rate performance of DDPCN was checked by the comparative analysis of voltage gap with Pt/C at various discharge currents. The voltage gap has increased from 7.6 mV to 18.1 mV as the current density increased from 5 to 50 mA/cm^2, which indicated the better conductivity of DDPCN than Pt/C (20%). Hence, DDPCN showed a better comprehensive performance than the Pt/C (20%) as the cathode electrode for Zn-air battery application.

As the air containing trace amount of molecular species (SO_x/NO_x) may affect the performance of zinc-air batteries. Therefore, the resistance of DDPCN as air-cathode towards small molecular poisons was monitored (Fig. 6a–f). The state-of-the-art Pt/C (Fig. 6b

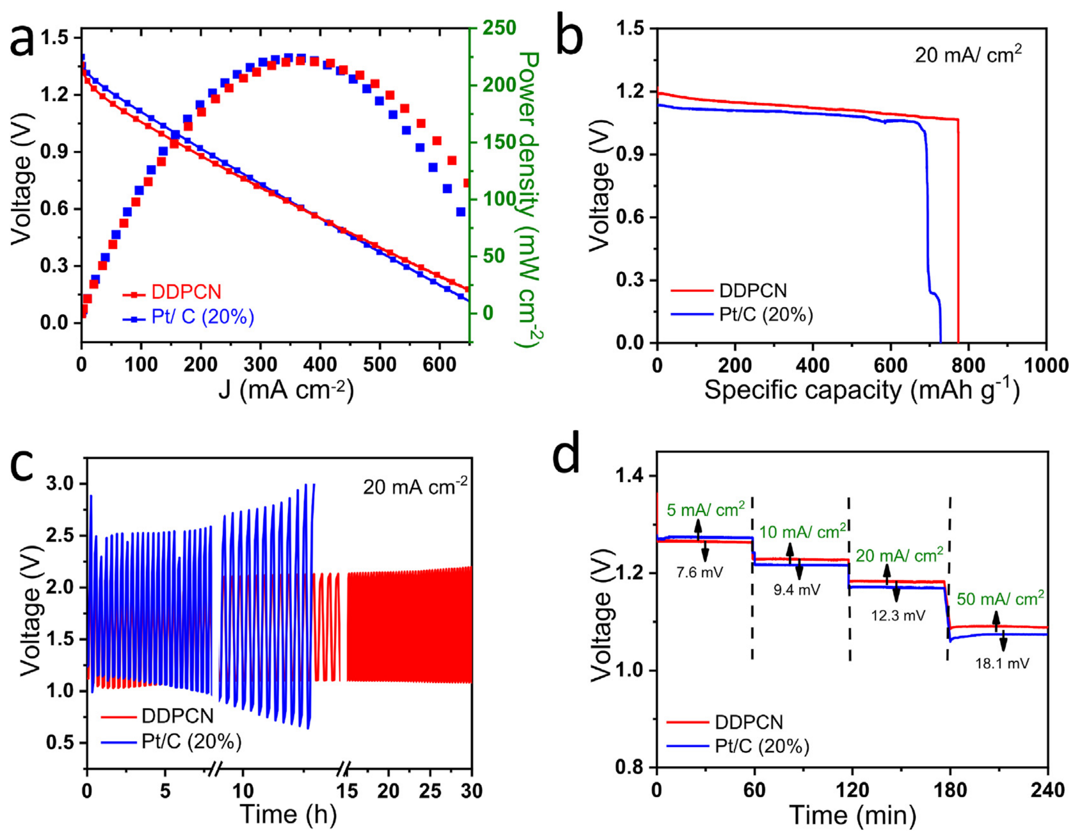

Fig. 5. The performance of Zinc-air battery based on cathode made of DDPCN and Pt/C (20%) catalysts, respectively; (a) Comparative analysis of discharge voltage curve (v–i) and the corresponding power density plot, (b) Specific capacitance curves obtained at 20 mA cm^{-2}, (c) Charge/discharge cycling curves at a current density of 20 mA cm^{-2} (5 min/cycle), (d) Galvanostatic discharge curves at 5, 10, 20, and 50 mA cm^{-2}. (A colour version of this figure can be viewed online.)

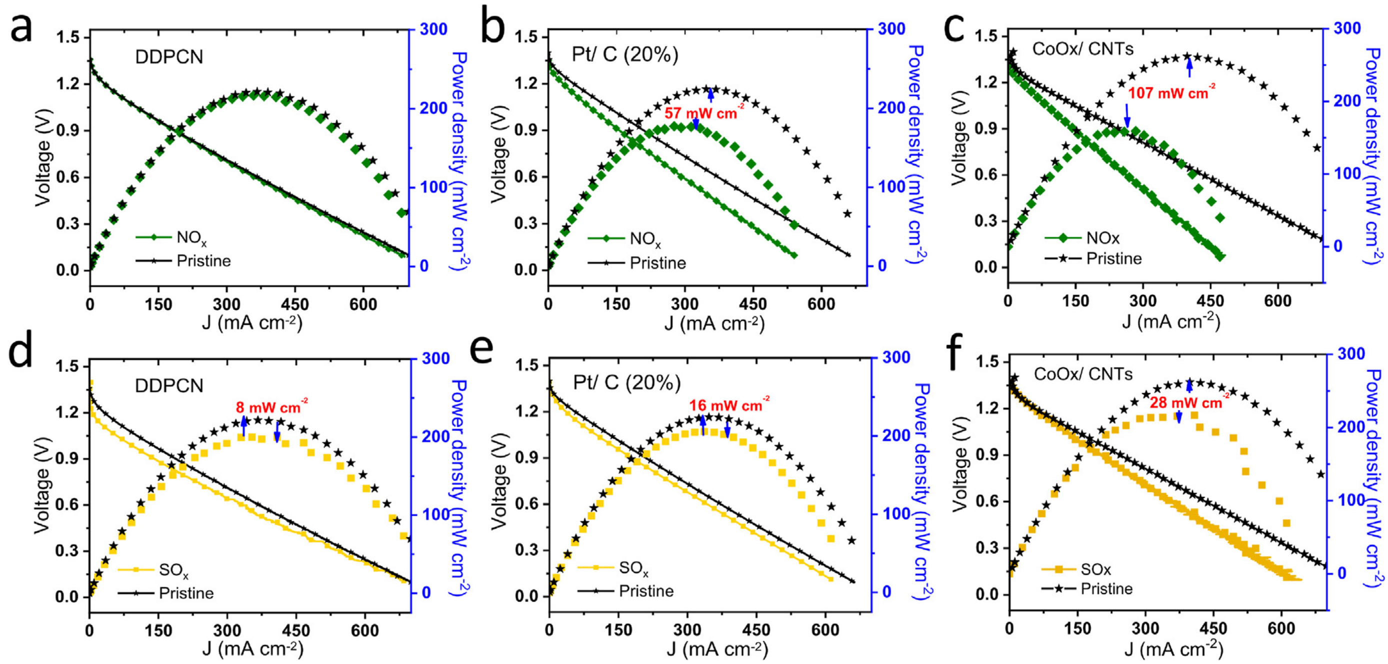

Fig. 6. Comparative analysis of discharge voltage curve (v–i) and the corresponding power density plot of Zinc-air battery test for DDPCN, Pt/C (20%) and CoO_x/CNTs under pristine conditions and in the presence of; (a–c) NO_x (50 mM of KNO_2), (d–f) SO_x (50 mM K_2SO_3). (A colour version of this figure can be viewed online.)

and e) and CoO_x/CNTs (Fig. 6c and f) were used as the cathode catalyst for comparative analysis. In the presence of SO_3^{2-} (50 mM K_2SO_3) and NO_2^- (50 mM KNO_2), the Zn-air battery displayed negligible performance change by using the DDPCN as a catalyst while drastic performance degradation was shown by using the Pt/C (20%) and CoO_x/CNTs as the catalysts. Especially, in the presence of NO_2^- species, the peak power density for Pt/C (20%) and CoO_x/CNTs decreased over 57 mW cm^{-2} and 107 mW cm^{-2}, which are around 25% and 40% decay of performances. Such large degradation would greatly impede their real applications. These results signify the potential of DDPCN as the cathode catalyst for Zn-air battery application compared to other precious and non-precious metallic electrocatalysts, such as Pt/C and CoO_x/CNT. However, in-depth studies are needed to further explore the mechanism behind the antipoisoning effect of P, N co-doped nanocarbon and the poisoning effect of PMCs and NPMCs in alkaline medium.

3. Summary

An efficient DDPCN catalyst for ORR was synthesized by a facile polymerization and pyrolysis procedure. The as obtained material has a mesoporous structure and a large specific surface area (894 m^2/g). Such a microstructure could expose more active sites on the surfaces and facilitates the mass transfer. In the meantime, P doping increased the N contents in the DDPCN and the ratio of pyridinic N inside, boosting the ORR performance. Moreover, the newly formed P–C–N structure could impede the blocking of catalytic sites by the anionic poison species due to the weaken polarization and steric hindrance effect by N/P co-doping. Therefore, DDPCN showed excellent ORR performance with high $E_{1/2}$ value (0.87 V), low Tafel slop (72 mV/dec), long cycling stability and good resistance towards the SO_3^{2-} and NO_2^-, which stands as a milestone for ORR catalysts with the best comprehensive performance. For Zn-air battery applications, DDPCN showed a peak power density of 224 mW/cm^2, energy density of 874 Wh kg^{-1}, and open circuit voltage of 1.48 V, which are comparable or slightly better than the Pt/C catalyst. Most importantly, DDPCN showed negligible performance degradation in the presence of SO_3^{2-} and NO_2^- for Zn-air battery, while sharp performance degradation up to 25% and 40% was shown by typical catalysts, such as Pt/C and CoO_x/CNT. This work may open up a new avenue to use the nonmetallic catalysts for Zn-air battery applications, which could exclude the poisoning effect in metal containing catalysts.

Declaration of competing interest

The authors declare that they have no known competing financial interests or personal relationships that could have appeared to influence the work reported in this paper.

CRediT authorship contribution statement

Tayyaba Najam: Data curation, Formal analysis, Writing - original draft. **Syed Shoaib Ahmad Shah:** Formal analysis, Supervision. **Hassan Ali:** Resources, Methodology. **Zhaoqi Song:** Data curation, Formal analysis. **Haohao Sun:** Data curation, Formal analysis. **Zhengchun Peng:** Funding acquisition, Supervision, Writing - review & editing. **Xingke Cai:** Funding acquisition, Supervision, Writing - review & editing.

Acknowledgement

This work thanks financial supports from the Science and Technology Innovation Commission of Shenzhen (KQTD20170810105439418, JCYJ20170818091233245), Guangdong University Young Talents Project (No. 2018KQNCX218), NTUT-SZU Joint Research Program (No. 2019001) and Research Start-Up Fund of Shenzhen University (No. 2019017).

Appendix A. Supplementary data

Supplementary data to this article can be found online at https://doi.org/10.1016/j.carbon.2020.03.036.

References

[1] F. Cheng, J. Chen, Metal–air batteries: from oxygen reduction electrochemistry to cathode catalysts, Chem. Soc. Rev. 41 (2012) 2172–2192.
[2] R. Cao, J.-S. Lee, M. Liu, J. Cho, Recent progress in non-precious catalysts for metal-air batteries, Adv. Energy Mater. 2 (2012) 816–829.
[3] T. Najam, S.S. Ahmad Shah, W. Ding, J. Deng, Z. Wei, Enhancing by nano-engineering: hierarchical architectures as oxygen reduction/evolution reactions for zinc-air batteries, J. Power Sources 438 (2019), 226919.
[4] M.K. Aslam, S.S.A. Shah, T. Najam, S. Li, C. Chen, Decoration of cobalt/iron oxide nanoparticles on N-doped carbon nanosheets: electrochemical performances for lithium-ion batteries, J. Appl. Electrochem. 49 (2019) 433–442.
[5] Z. Yang, J. Zhang, M.C.W. Kintner-Meyer, X. Lu, D. Choi, J.P. Lemmon, J. Liu, Electrochemical energy storage for green grid, Chem. Rev. 111 (2011) 3577–3613.
[6] B. Dunn, H. Kamath, J.-M. Tarascon, Electrical energy storage for the grid: a battery of choices, Science 334 (2011) 928–935.
[7] X.N. Xie, Y. Wang, Q. Wang, K.P. Loh, A percolating membrane with superior polarization and power retention for rechargeable energy storage, Adv. Mater. 24 (2012) 76–81.
[8] G. Wu, P. Zelenay, Nanostructured nonprecious metal catalysts for oxygen reduction reaction, Acc. Chem. Res. 46 (2013) 1878–1889.
[9] M. Lefèvre, E. Proietti, F. Jaouen, J.-P. Dodelet, Iron-based catalysts with improved oxygen reduction activity in polymer electrolyte fuel cells, Science 324 (2009) 71–74.
[10] M.K. Debe, Electrocatalyst approaches and challenges for automotive fuel cells, Nature 486 (2012) 43–51.
[11] Z.-L. Wang, D. Xu, J.-J. Xu, X.-B. Zhang, Oxygen electrocatalysts in metal-air batteries: from aqueous to nonaqueous electrolytes, Chem. Soc. Rev. 43 (2014) 7746–7786.
[12] Y. Li, H. Dai, Recent advances in zinc–air batteries, Chem. Soc. Rev. 43 (2014) 5257–5275.
[13] T. Najam, S.S. Ahmad Shah, W. Ding, Z. Ling, L. Li, Z. Wei, Electron penetration from metal core to metal species attached skin in nitrogen-doped core-shell catalyst for enhancing oxygen evolution reaction, Electrochim. Acta 327 (2019), 134939.
[14] S.S. Ahmad Shah, T. Najam, C. Cheng, S. Chen, R. Xiang, L. Peng, L. Lu, W. Ding, Z. Wei, Design and synthesis of conductive carbon polyhedrons enriched with Mn-Oxide active-centres for oxygen reduction reaction, Electrochim. Acta 272 (2018) 169–175.
[15] S.S.A. Shah, T. Najam, M.K. Aslam, M. Ashfaq, M.M. Rahman, K. Wang, P. Tsiakaras, S. Song, Y. Wang, Recent advances on oxygen reduction electrocatalysis: correlating the characteristic properties of metal organic frameworks and the derived nanomaterials, Appl. Catal. B Environ. (2019), 118570.
[16] A. Mahata, A.S. Nair, B. Pathak, Recent advancements in Pt-nanostructure-based electrocatalysts for the oxygen reduction reaction, Catal. Sci. Technol. 9 (2019) 4835–4863.
[17] C. Li, H. Tan, J. Lin, X. Luo, S. Wang, J. You, Y.-M. Kang, Y. Bando, Y. Yamauchi, J. Kim, Emerging Pt-based electrocatalysts with highly open nanoarchitectures for boosting oxygen reduction reaction, Nano Today 21 (2018) 91–105.
[18] Y.-J. Wang, N. Zhao, B. Fang, H. Li, X.T. Bi, H. Wang, Carbon-supported Pt-based alloy electrocatalysts for the oxygen reduction reaction in polymer electrolyte membrane fuel cells: particle size, shape, and composition manipulation and their impact to activity, Chem. Rev. 115 (2015) 3433–3467.
[19] Q. He, B. Shyam, M. Nishijima, D. Ramaker, S. Mukerjee, Mitigating phosphate anion poisoning of cathodic Pt/C catalysts in phosphoric acid fuel cells, J. Phys. Chem. C 117 (2013) 4877–4887.
[20] T. Najam, S.S.A. Shah, W. Ding, Z. Wei, Role of P-doping in antipoisoning: efficient MOF-derived 3D hierarchical architectures for the oxygen reduction reaction, J. Phys. Chem. C 123 (2019) 16796–16803.
[21] S.S.A. Shah, L. Peng, T. Najam, C. Cheng, G. Wu, Y. Nie, W. Ding, X. Qi, S. Chen, Z. Wei, Monodispersed Co in mesoporous polyhedrons: fine-tuning of ZIF-8 structure with enhanced oxygen reduction activity, Electrochim. Acta 251 (2017) 498–504.
[22] M.K. Aslam, S.S.A. Shah, S. Li, C. Chen, Kinetically controlled synthesis of MOF nanostructures: single-holed hollow core–shell ZnCoS@Co_9S_8/NC for ultra-high performance lithium-ion batteries, J. Mater. Chem. A 6 (2018) 14083–14090.
[23] X. Li, G. Liu, B.N. Popov, Activity and stability of non-precious metal catalysts for oxygen reduction in acid and alkaline electrolytes, J. Power Sources 195 (2010) 6373–6378.
[24] V. Goellner, C. Baldizzone, A. Schuppert, M.T. Sougrati, K. Mayrhofer, F. Jaouen, Degradation of Fe/N/C catalysts upon high polarization in acid medium, Phys. Chem. Chem. Phys. 16 (2014) 18454–18462.
[25] U.I. Kramm, M. Lefèvre, P. Bogdanoff, D. Schmeißer, J.-P. Dodelet, Analyzing structural changes of Fe–N–C cathode catalysts in PEM fuel cell by Mößbauer spectroscopy of complete membrane electrode assemblies, J. Phys. Chem. Lett. 5 (2014) 3750–3756.
[26] A. Pozio, R.F. Silva, M. De Francesco, L. Giorgi, Nafion degradation in PEFCs from end plate iron contamination, Electrochim. Acta 48 (2003) 1543–1549.
[27] C.H. Choi, C. Baldizzone, J.-P. Grote, A.K. Schuppert, F. Jaouen, K.J.J. Mayrhofer, Stability of Fe-N-C catalysts in acidic medium studied by operando spectroscopy, Angew. Chem. Int. Ed. 54 (43) (2015) 12753–12757.
[28] S.S.A. Shah, T. Najam, C. Cheng, L. Peng, R. Xiang, L. Zhang, J. Deng, W. Ding, Z. Wei, Exploring Fe-N_x for peroxide reduction: template-free synthesis of Fe-N_x traumatized mesoporous carbon nanotubes as an ORR catalyst in acidic and alkaline solutions, Chem. Eur J. 24 (2018) 10630–10635.
[29] K. Mamtani, D. Jain, D. Zemlyanov, G. Celik, J. Luthman, G. Renkes, A.C. Co, U.S. Ozkan, Probing the oxygen reduction reaction active sites over nitrogen-doped carbon nanostructures (CN_x) in acidic media using phosphate anion, ACS Catal. 6 (2016) 7249–7259.
[30] D. Malko, A. Kucernak, T. Lopes, Performance of Fe–N/C oxygen reduction electrocatalysts toward NO_2^-, NO, and NH_2OH electroreduction: from fundamental insights into the active center to a new method for environmental nitrite destruction, J. Am. Chem. Soc. 138 (2016) 16056–16068.
[31] J. Zhang, L. Dai, Heteroatom-doped graphitic carbon catalysts for efficient electrocatalysis of oxygen reduction reaction, ACS Catal. 5 (2015) 7244–7253.
[32] Y. Zheng, Y. Jiao, M. Jaroniec, Y. Jin, S.Z. Qiao, Nanostructured metal-free electrochemical catalysts for highly efficient oxygen reduction, Small 8 (2012) 3550–3566.
[33] B. He, F. Liu, S. Yan, Temperature-directed growth of highly pyridinic nitrogen doped, graphitized, ultra-hollow carbon frameworks as an efficient electrocatalyst for the oxygen reduction reaction, J. Mater. Chem. A 5 (2017) 18064–18070.
[34] Z. Yang, H. Nie, X.a. Chen, X. Chen, S. Huang, Recent progress in doped carbon nanomaterials as effective cathode catalysts for fuel cell oxygen reduction reaction, J. Power Sources 236 (2013) 238–249.
[35] J. Zhang, Z. Zhao, Z. Xia, L. Dai, A metal-free bifunctional electrocatalyst for oxygen reduction and oxygen evolution reactions, Nat. Nanotechnol. 10 (2015) 444–452.
[36] J. Zhang, L. Qu, G. Shi, J. Liu, J. Chen, L. Dai, N,P-codoped carbon networks as efficient metal-free bifunctional catalysts for oxygen reduction and hydrogen evolution reactions, Angew. Chem. Int. Ed. 55 (2016) 2230–2234.
[37] J. Zhang, L. Dai, Nitrogen, phosphorus, and fluorine tri-doped graphene as a multifunctional catalyst for self-powered electrochemical water splitting, Angew. Chem. Int. Ed. 55 (2016) 13296–13300.
[38] D. Guo, R. Shibuya, C. Akiba, S. Saji, T. Kondo, J. Nakamura, Active sites of nitrogen-doped carbon materials for oxygen reduction reaction clarified using model catalysts, Science 351 (2016) 361.
[39] C. Zhang, R. Hao, H. Liao, Y. Hou, Synthesis of amino-functionalized graphene as metal-free catalyst and exploration of the roles of various nitrogen states in oxygen reduction reaction, Nano Energy 2 (2013) 88–97.
[40] I.O. Maciel, J. Campos-Delgado, E. Cruz-Silva, M.A. Pimenta, B.G. Sumpter, V. Meunier, F. López-Urías, E. Muñoz-Sandoval, H. Terrones, M. Terrones, A. Jorio, Synthesis, electronic structure, and Raman scattering of phosphorus-doped single-wall carbon nanotubes, Nano Lett. 9 (2009) 2267–2272.
[41] D.-W. Wang, D. Su, Heterogeneous nanocarbon materials for oxygen reduction reaction, Energy Environ. Sci. 7 (2014) 576–591.
[42] T. Najam, S.S.A. Shah, W. Ding, J. Jiang, L. Jia, W. Yao, L. Li, Z. Wei, An efficient anti-poisoning catalyst against SO_x, NO_x, and PO_x: P, N-doped carbon for oxygen reduction in acidic media, Angew. Chem. Int. Ed. 57 (2018) 15101–15106.
[43] S. Brunauer, L.S. Deming, W.E. Deming, E. Teller, On a theory of the van der Waals adsorption of gases, J. Am. Chem. Soc. 62 (1940) 1723–1732.
[44] D.-S. Yang, D. Bhattacharjya, S. Inamdar, J. Park, J.-S. Yu, Phosphorus-doped ordered mesoporous carbons with different lengths as efficient metal-free electrocatalysts for oxygen reduction reaction in alkaline media, J. Am. Chem. Soc. 134 (2012) 16127–16130.